MICROBIOLOGY

A centimeter-long bacterium with DNA contained in metabolically active, membrane-bound organelles

Jean-Marie Volland[1,2]*†, Silvina Gonzalez-Rizzo[3]†, Olivier Gros[3,4]*†, Tomáš Tyml[1,2], Natalia Ivanova[1], Frederik Schulz[1], Danielle Goudeau[1], Nathalie H. Elisabeth[5], Nandita Nath[1], Daniel Udwary[1], Rex R. Malmstrom[1], Chantal Guidi-Rontani[6], Susanne Bolte-Kluge[7], Karen M. Davies[5,8]‡, Maïtena R. Jean[3], Jean-Louis Mansot[4], Nigel J. Mouncey[1], Esther R. Angert[9], Tanja Woyke[1,2,10]*, Shailesh V. Date[2,11,12]*

Cells of most bacterial species are around 2 micrometers in length, with some of the largest specimens reaching 750 micrometers. Using fluorescence, x-ray, and electron microscopy in conjunction with genome sequencing, we characterized *Candidatus* (*Ca.*) Thiomargarita magnifica, a bacterium that has an average cell length greater than 9000 micrometers and is visible to the naked eye. These cells grow orders of magnitude over theoretical limits for bacterial cell size, display unprecedented polyploidy of more than half a million copies of a very large genome, and undergo a dimorphic life cycle with asymmetric segregation of chromosomes into daughter cells. These features, along with compartmentalization of genomic material and ribosomes in translationally active organelles bound by bioenergetic membranes, indicate gain of complexity in the *Thiomargarita* lineage and challenge traditional concepts of bacterial cells.

Bacteria and archaea are taxonomically and metabolically the most diverse and abundant organisms on Earth, but with only a small fraction of them isolated in culture, we remain grossly ignorant of their biology (*1*). Although most model bacteria and archaea are small, some remarkably large cells, referred to as giant bacteria, are evident in at least four phyla (*2*), and have cellular sizes in the range of tens or even hundreds of micrometers (*3*, *4*). Some exceptional members of the sulfur-oxidizing gammaproteobacteria *Thiomargarita namibiensis*, for instance, are known to reach up to 750 μm (average size: 180 μm) (*4*–*6*). Such bacterial giants raise the question of whether other lineages of previously unidentified macrobacteria might exist.

Here, we describe a sessile filamentous *Thiomargarita* species from a marine sulfidic environment that is larger than all other known giant bacteria by ~50-fold. Our multifaceted imaging analyses revealed massive polyploidy and a dimorphic developmental cycle in which genome copies are asymmetrically segregated into apparent dispersive daughter cells. We show that centimeter-long *Thiomargarita* filaments represent individual cells with genetic material and ribosomes compartmentalized into a metabolically active, membrane-bound organelle. Sequencing and analysis of genomes from five single cells revealed insights into distinct cell division and cell elongation mechanisms. These cellular features likely allow the organism to grow to an unusually large size and circumvent some of the biophysical and bioenergetic limitations on growth. In reference to its exceptional size, we propose to name this species *Thiomargarita magnifica*, which is hereafter referred to as *Candidatus* (*Ca.*) Thiomargarita magnifica.

Ca. T. magnifica is a centimeter-long, single bacterial cell

Some large sulfur bacteria (LSB) form very long filaments that may reach several centimeters in length but are composed of thousands of individual cells that do not exceed 200 μm (*7*–*10*). We observed seasonal "bouquets" of centimeter-long white filamentous *Thiomargarita* cells attached to sunken leaves of *Rhizophora mangle* (fig. S1) in shallow tropical marine mangroves from Guadeloupe, Lesser Antilles. *Thiomargarita* spp. are sulfur-oxidizing gammaproteobacteria known to be morphologically diverse and to display polyphenism (*11*). The morphology of the filaments observed in Guadeloupe resembled those of sessile *Thiomargarita*-like cells reported from deep-sea methane seeps (*12*). They had a stalk-like shape for most of their length and constricted gradually toward the apical end, forming buds (Fig. 1, A to E). In contrast to relatives that live buried in sediment, these filaments were smooth in appearance and free of epibiotic bacteria or any extracellular mucus matrix (figs. S1 and S2) (*11*). Budding filaments had an average length of 9.72 ± 4.25 mm, and only the most apical constrictions closed completely to form one to four separate, rod-shaped cells of 0.21 ± 0.05 mm. We also noted that some filaments reached a length of 20.00 mm (Fig. 1A and figs. S1 and S3), much larger than any previously described single-celled prokaryote.

To further characterize *Ca.* T. magnifica cells, we highlighted membranes using osmium tetroxide or the fluorescent dye FM 1-43X, and visualized entire filaments in three dimensions (3D) with hard x-ray tomography (n = 4; Fig. 1C and movies S1 and S2) and confocal laser scanning microscopy (CLSM) (n = 6; Fig. 1, C and D, and movie S3). Filament sections (up to 850.6 μm in length) were visualized with transmission electron microscopy (TEM) (n = 15; Fig. 1, E to G, and fig. S5). All techniques consistently showed that each filament was one continuous cell for nearly its entire length, with no division septa, including the partial constrictions toward the apical pole. Only the most apical few buds were separated from the filament by a closed constriction and these represented daughter cells (Fig. 1, fig. S5, and movies S1 to S4).

Similar to other LSB, *Ca.* T. magnifica cells has a large central vacuole that reduces the cytoplasmatic space. This may minimize growth limitation due to the reliance on chemical diffusion because bacteria lack an active intracellular transport system (*2*, *4*). In *Ca.* T. magnifica, the central vacuole was continuous along the whole filament and accounted for 73.2 ± 7.5% (n = 4) of the total volume (Fig. 1, D and E; fig. S5; and table S2). The cytoplasm was 3.34 ± 1.48 μm thick and was constrained to the periphery of the cell, so it was preserved from such chemical diffusion limitations (Fig. 1, E and F, and fig. S5) (*4*).

Within the cytoplasm, TEM revealed numerous lucent vesicles 2.40 ± 1.03 μm in diameter, which corresponded to the refractile granules observed with bright-field microscopy and represented sulfur granules, as shown by energy dispersive x-ray spectroscopy (Fig. 1F, figs. S5 and S13, and supplementary text). The cytoplasm of *Ca.* T. magnifica appeared to contain many electron-dense membrane-bound compartments 1.31 ± 0.70 μm in diameter (Fig. 1, F and G). Similar structures have

[1]Department of Energy Joint Genome Institute, Lawrence Berkeley National Laboratory, Berkeley, CA, USA. [2]Laboratory for Research in Complex Systems, Menlo Park, CA, USA. [3]Institut de Systématique, Evolution, Biodiversité, Université des Antilles, Muséum National d'Histoire Naturelle, CNRS, Sorbonne Université, EPHE, Campus de Fouillole, Pointe-à-Pitre, France. [4]Centre Commun de Caractérisation des Matériaux des Antilles et de la Guyane, Université des Antilles, UFR des Sciences Exactes et Naturelles, Pointe-à-Pitre, Guadeloupe, France. [5]Department of Energy Molecular Biophysics and Integrated Bioimaging, Lawrence Berkeley National Laboratory, Berkeley, CA, USA. [6]Institut de Systématique, Evolution, Biodiversité CNRS UMR 7205, Museum National d'Histoire Naturelle, Paris, France. [7]Sorbonne Universités, UPMC Univ. Paris 06, CNRS FRE3631, Institut de Biologie Paris Seine, Paris, France. [8]Department of Molecular and Cell Biology, University of California, Berkeley, USA. [9]Cornell University, College of Agriculture and Life Sciences, Department of Microbiology, Ithaca, NY, USA. [10]University of California Merced, School of Natural Sciences, Merced, CA, USA. [11]University of California San Francisco, San Francisco, CA, USA. [12]San Francisco State University, San Francisco, CA, USA.
***Corresponding author. Email: jvolland@lbl.gov (J.-M.V.); Olivier.Gros@univ-antilles.fr (O.G.); twoyke@lbl.gov (T.W.); shailesh.date@lrc.systems (S.V.D.)**
†These authors contributed equally to this work.
‡Present address: Electron Bio-Imaging Centre, Diamond Light Source, Harwell Science and Innovation Campus, Didcot, UK.

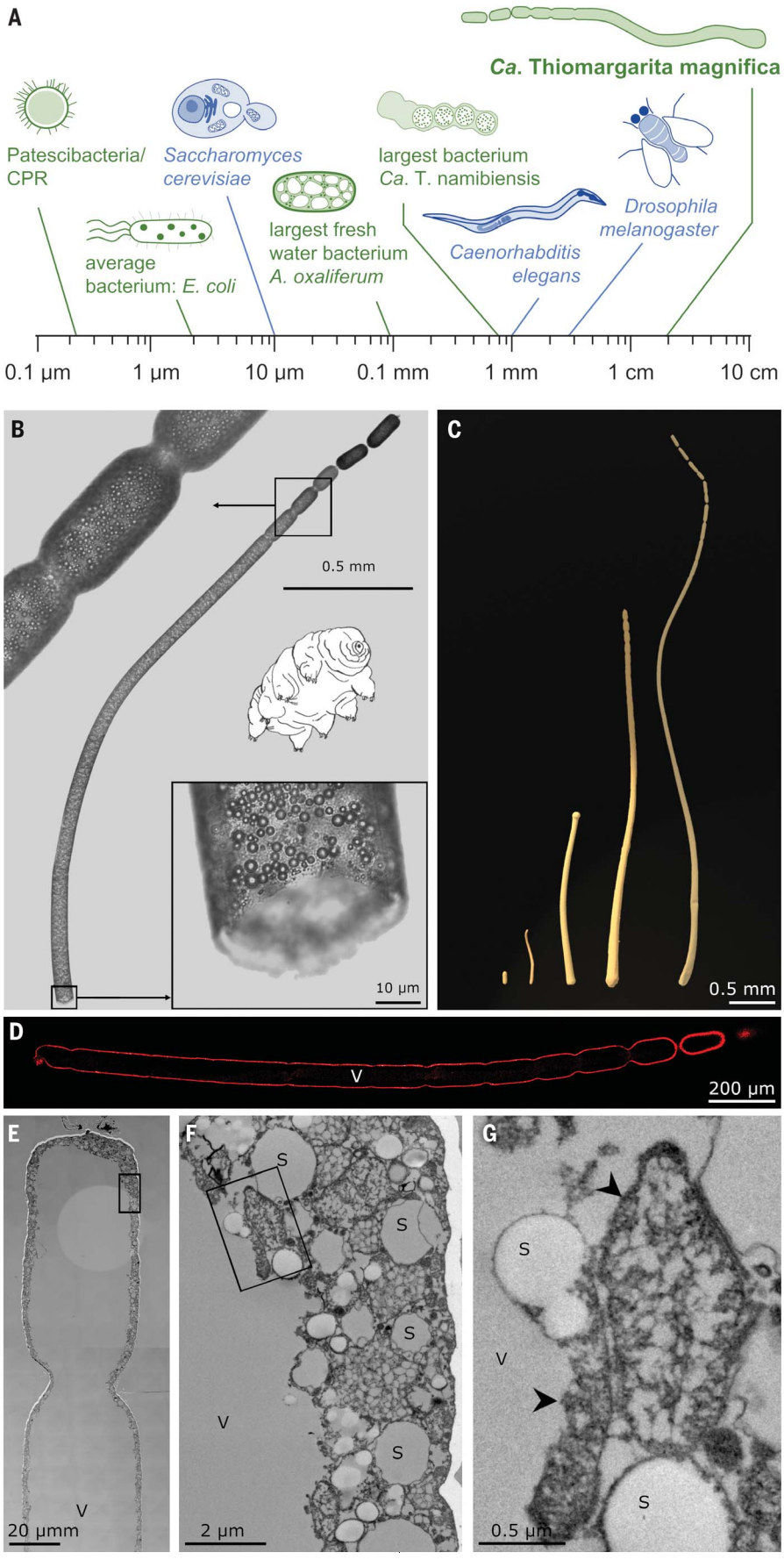

occasionally been observed in other LSB and have been referred to as "blebs of cytoplasm," "putative endobionts," "intracytoplasmic structures which appear to contain nuclear material," or "membrane-enclosed cytoplasmic compartments with ribosomes and DNA fibrils," but their nature and function remained elusive in these primarily ultrastructural studies (*7*, *10*, *13*). We hypothesized that some of these membrane-bound compartments within the cytoplasm may contain dispersed genomic material because polyploidy is evident in many giant bacteria (*2*, *14*, *15*).

DNA and ribosomes within a membrane-bound bacterial organelle

Although bacteria were once presumed to be uncompartmentalized "bags of enzymes," recent studies have revealed the presence of organelles with functions as diverse as anaerobic ammonium oxidation, photosynthesis, and magnetic orientation (*16*). No bacteria or archaea are known to unambiguously segregate their genetic material in the manner of eukaryotes. There is, however, some evidence of membrane-bound nucleoids in one member of the Atribacteria, which has a compartment containing DNA that occupies most of the cell's volume (*17*). Plancotomycetes such as *Gemmata obscuriglobus* also have cytosolic

Fig. 1. Morphology and ultrastructure of *Ca.* T. magnifica. (**A**) Size comparison of selected bacterial (green) and eukaryotic (blue) model systems on a log scale. (**B**) Light microscopy montage of the upper half of a *Ca.* T. magnifica cell, with a broken basal part revealing a tube-like morphology due to the large central vacuole and numerous spherical intracellular sulfur granules (a tardigrade is shown for scale). (**C**) 3D rendering of segmented cells from hard x-ray tomography (movies S1, S2, and S6) and CLSM (movie S3) putatively at various stages of the developmental cycle. From left to right, 3D rendered cells *D*, *B*, *F*, *G*, and *D* (table S2). Note that the smallest stage corresponds to the cell *D* terminal segment and was added to the left for visualization purposes. (**D**) CLSM observation of cell *K* (table S2) after fluorescent labeling of membranes with FM 1-43X showing the continuity of the cell from the basal pole to the first complete constriction at the apical end. (**E**) TEM montage of the apical constriction of a cell, with the cytoplasm constrained to the periphery. (**F**) Higher magnification of the area marked in (E), with sulfur granules and pepins at various stages of development. (**G**) Higher magnification of the area marked in (F) showing two pepins (arrowheads). S, sulfur granule; V, vacuole.

compartments with DNA, and recent work has shown that these compartments represent deep invaginations of a Gram-negative cytoplasmic membrane rather than a closed, membrane-bound organelle (*16*).

4′,6-Diamidino-2-phenylindole (DAPI) staining revealed that the DNA in *Ca*. T. magnifica cells was concentrated in the membrane-bound compartments (Fig. 2, H to J, and fig. S6). Although we did not observe any connection of these compartments to the cell envelope, their mechanism of formation, which may include cell membrane invagination, is yet to be studied. They also harbored electron-dense structures 10 to 20 nm in size, similar to signatures of

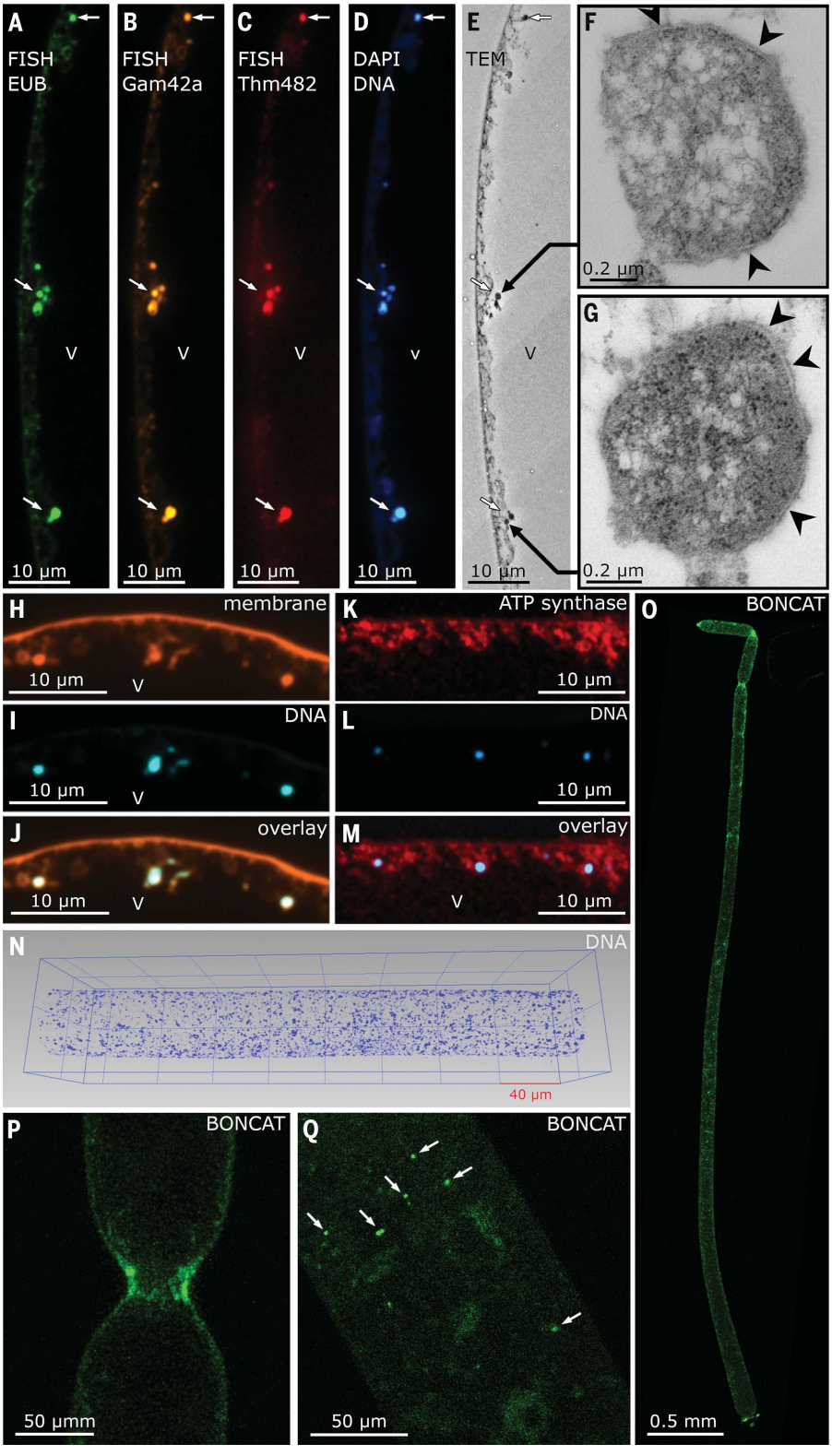

Fig. 2. Characterization of the pepin organelles by FISH and correlative TEM, as well as membrane and DNA staining, immunohistochemistry, and BONCAT. (**A** to **D**) FISH of pepins (arrows) in the cytoplasm of *Ca*. T. magnifica (class gammaproteobacteria). Pepins are labeled with the general bacterial probe EUB labeled with Alexa Fluor 488 [(A), green], the gammaproteobacteria-specific probe Gam42a labeled with Cy3 [(B), yellow], and the *Thiomargarita*-specific probe Thm482 labeled with Cy5 [(C), red] and with DAPI [(D), blue] (see the supplementary text for details). (**E**) TEM of a serial thin section consecutive to the semithin section used for FISH. The FISH- and DAPI-positive pepins appear as electron-dense organelles under TEM. (**F** and **G**) Pepins from (E) under higher magnification. Pepins are delimited by a membrane (arrowheads) and contain numerous ribosomes that appear as small, electron-dense granules throughout the sections of the pepins. (**H** to **J**) Fluorescent labeling of membranes using FM 1-43X (H) and of DNA using DAPI (I) and overlay (J) on a cross section of a cell. The pepins labeled with DAPI are also labeled with the dye FM 1-43X, confirming the presence of a membrane. (**K** to **M**) Visualization of ATP synthase localization using immunohistochemistry. Anti–ATP synthase antibodies label (K) reveals the presence of bioenergetic membranes around pepins [labeled with DAPI in (L)] and throughout the cytoplasm. (**N**) 3D visualization of a central portion of a cell after DAPI staining (blue) showing the multitude of DNA clusters spread throughout the cytoplasm (cell *M*; table S2 and movie S5). (**O** to **Q**) Translational activity revealed by BONCAT showing active protein biosynthesis within an entire cell, including hotspots at constriction sites and pepins [enlarged in (P) and (Q), respectively].

ribosomes (Fig. 2, F and G, and fig. S6, G to K). Fluorescence in situ hybridization (FISH) with probes specifically targeting ribosomal RNA sequences of *Thiomargarita* confirmed that ribosomes were indeed present and were concentrated in these membrane-bound structures (Fig. 2, A to G, and figs. S7 to S9) and spread throughout the entire cell, including the apical buds (fig. S9). This compartmentalization of DNA and ribosomes is reminiscent of the genomic nuclear compartmentalization in eukaryotes. By analogy with pips, the numerous small seeds in fruits such as watermelon or kiwi, we propose to name this bacterial organelle a *pepin* (singular *pepin*, plural *pepins*: from vulgar Latin *pép*, an expressive creation used to express smallness).

Cytoplasmic localization of bioenergetic membranes and translational activity

Adenosine triphosphate (ATP), the principal and universal energy currency of cells, is produced by ATP synthase, a molecular machine embedded in bioenergetic membranes and powered by proton motive force. Bacterial and archaeal ATP synthases are often observed to be localized to the cell envelope, in contrast to eukaryotes, in which ATP is generated by mitochondria. This cell envelope localization potentially constrains bacterial cell size because of the surface-to-volume ratio required to satisfy energy needs; a theoretical maximum cell size of ~10^{-14} m^3 has been estimated recently (*18*). Giant *Thiomargarita* cells are often cited as being exceptions to such energetic constraints and are thought to rely on their cell surface for ATP production (*19*–*21*). We used immunohistochemistry to assess the localization of ATP synthase in *Ca.* T. magnifica. We observed the distribution of ATP synthases around pepins and throughout the complex membrane network of the entire cytoplasm, but they were absent from the outer cell envelope (Fig. 2, K to M, and fig. S20).

To examine the localization of activity throughout the whole cell, we used bioorthogonal noncanonical amino acid tagging (BONCAT) to detect protein biosynthesis (*22*). Live filaments incubated with a clickable amino acid analog were labeled throughout (Fig. 2O and fig. S10). Consistent with the detection of ribosomes by FISH and TEM, BONCAT showed protein biosynthesis activity in small, round-shaped areas that were similar to pepins in size and localization, but not all pepins appeared to be labeled (Fig. 2Q and fig. S10D). Labeled hotspots were also observed at the site of constriction in the apical part of cells, suggesting higher translational activity or concentration of newly synthesized proteins in these areas (Fig. 2P). The establishment of stable continuous laboratory cultures of *Ca.* T. magnifica will likely be necessary to undertake detailed studies of the formation, biochemistry, and functions of pepins.

Based on these data, the metabolically active biovolume of *Ca.* T. magnifica (excluding the central vacuole) is two orders of magnitude above the predicted maximum mentioned above (table S2). This does not appear to contradict previous studies; indeed, such models have excluded bacteria with structural adaptations such as endomembrane systems and slower growth rates, which allow much larger cell volumes (*18*). Whereas most bacteria have doubling times ranging from minutes to hours, *Ca.* T. magnifica may be similar to other *Thiomargarita* species, which require up to 2 weeks to produce daughter cells (*5*). The predicted maximum volume of bacteria assumes binary fission as a division mode, but *Ca.* T. magnifica does not have to double its volume to produce a daughter cell because only a small portion of the apex constricts and detaches from the mother cell.

A highly polyploid cell with a large genome

All previously described giant bacteria are polyploid (*2*, *3*, *14*), meaning that their cells contain large numbers of genome copies ranging from tens to tens of thousands that are dispersed throughout the cell, supporting the local need for molecular machineries and overall cellular growth (*15*, *23*, *24*). Polyploidy has been shown to decrease the selective pressure on genes, allowing intracellular gene duplication, reassortment, and divergence, and to lead to extreme intracellular genetic diversity in some LSB (*25*). Conversely, polyploidy may allow balancing of genome copies through homologous recombination and support a high level of genome conservation (*26*). *Ca.* T. magnifica, like all bacterial giants, appeared to be polyploid; counts of DAPI-stained DNA clusters on three CLSM 3D datasets suggested an average of 36,880 ± 7956 genome copies per millimeter of filament (737,598 ± 159,115 for a fully grown 2-cm cell; see table S2, Fig. 2N, movie S5, and details in supplementary text). With its number of genome copies being one order of magnitude above that of other giant bacteria (*2*, *24*), *Ca.* T. magnifica accounts for the highest estimated number of genome copies within a single cell. Understanding the mechanisms underlying the regulation of such a large number of genome copies will require additional work.

To genomically characterize *Ca.* T. magnifica, we amplified, sequenced, and assembled the DNA of five individual cells collected from a single sunken leaf (tables S3 and S4). All five draft genomes were highly similar to each other, with an average nucleotide identity >99.5% (table S5). Although extreme intracellular genetic diversity has been shown in some LSB (*25*), our variant analysis of DNA sequences recovered from a single cell revealed a largely homogenous genome population (1.22 ± 0.18 single-nucleotide polymorphisms/100 kbp; table S6) (*27*), which is similar to other polyploid bacteria (*26*, *28*). The *Ca.* T. magnifica genome assemblies were estimated to be nearly complete at 91.0 to 93.7%, with total sequence lengths between 11.5 and 12.2 Mb. This value is twice as large as the only other sequenced *Thiomargarita* species, *Ca.* T. nelsonii (*29*, *30*), and at the upper range of bacterial genome sizes; bacterial genomes are on average 4.21 ± 1.77 Mb (fig. S11). The *Ca.* T. magnifica genomes contained up to 11,788 genes (only half with a functional annotation; table S4), more than three times the median gene count of prokaryotes (3935 genes) (*31*). For comparison with eukaryotic organisms, *Ca.* T. magnifica has a genome as large as the baker's yeast *Saccharomyces cerevisiae* (12.1 Mb) and contains more genes than the model fungus *Aspergillus nidulans* (≈ 9500 genes).

Analysis of the *Ca.* T. magnifica genome revealed a large set of genes for sulfur oxidation and carbon fixation, suggesting chemoautotrophy, which is consistent with other evidence for thioautotrophy (figs. S12 to S14 and supplementary text). Like its sister lineage *Ca.* T. nelsonii, *Ca.* T. magnifica encoded a wide range of metabolic capabilities with one notable difference: It lacked nearly all genes involved in dissimilatory and assimilatory nitrate reduction and denitrification except for Nar and Nap nitrate reductases (fig. S12). This absence suggests that nitrate can solely be used as an electron acceptor to be reduced to nitrite, which is not further reduced (*29*, *30*) (see the supplementary text for extended genome analysis). The absence of epibiotic bacteria may be explained by the high number of genes encoding secondary metabolism. With 25.9% of sequences dedicated to biosynthetic gene clusters (Fig. 3A), the genome encoded dozens of modular nonribosomal peptide synthetase and polyketide synthase systems, hinting at numerous secondary metabolism pathways (similar to the Actinobacteria; see table S7) that are indicative of antibiotic or bioactive compound production (*32*).

Giant bacteria have been shown to repurpose their cell division machinery as an adaptation to extreme cell size (*33*). The *Ca.* T. magnifica genome also holds clues for its unusual cell morphology in the form of an atypical complement of cell division and elongation genes. Many genes that encode core cell division proteins, including the core components of Z ring assembly and regulation, FtsA, ZipA, and FtsE-FtsX, were lacking (Fig. 3B and table S8). By contrast, genes that encode the cytoskeletal protein FtsZ, which is part of the well-conserved *dcw* ("division and cell wall") operon and the core component of the Z ring, were conserved. Proteins ZapA, ZapB, and ZapD, which interact with FtsZ and regulate Z ring assembly, were likewise conserved

(*34*).The entire set of genes that encode late divisome proteins, including peptidoglycan polymerases FtsI and FtsW, as well as FtsQ, FtsL, FtsB, and FtsK, was absent from all *Ca.* Thiomargarita genomes (Fig. 3B, fig. S19, and table S8). In contrast to the conspicuous lack of cell division genes, a complete set of genes encoding cell elongation proteins was present, three of which, *mreD*, *rodZ*, and the peptidoglycan transpeptidase *mrdA*, have undergone recent duplications, with both copies located next to each other on the chromosome (Fig. 3B, figs. S16 to S18, and table S8) (*34*). It is possible that an increased number of cell elongation genes, coupled with the lack of key cell division genes, may be responsible for producing the unusually long filaments of *Ca.* T. magnifica (see the supplementary text).

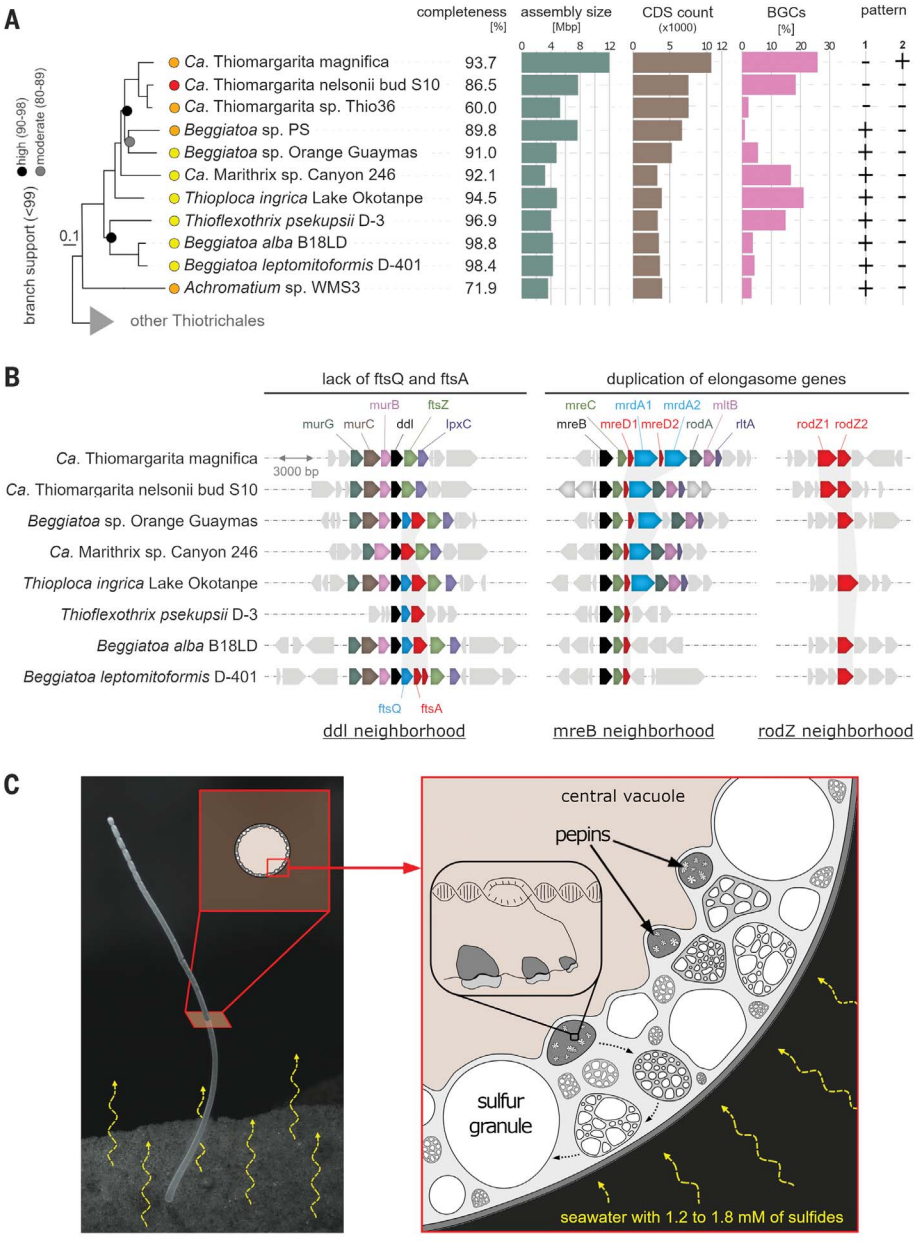

Fig. 3. Genome analysis and proposed model for the subcellular organization of *Ca.* T. magnifica. (**A**) Genome phylogenetic tree with added information about genome quality [red: low quality, orange: medium quality, and yellow: high quality (*46*)], estimated level of completeness, assembly size, coding sequence (CDS) count, and percentage of sequence dedicated to biosynthetic gene clusters (BGCs). Pattern 1 corresponds to "complete gene cluster for cell division of model bacteria." Pattern 2 corresponds to "*mreD*, *mrdA*, and *rodZ* genes are duplicated." (**B**) Gene neighborhoods centered on the *ddl*, *mreB*, and *rodZ* genes showing the incomplete set of divisome genes (lack of *ftsQ* and *ftsA*) in both *Thiomargarita* species, as well as the duplication of elongasome genes (*mreD*, *mrdA*, and *rodZ*) in *Ca.* T. magnifica. Note that the *Beggiatoa* sp. PS, *Achromatium* sp. WMS3, and *Ca.* Thiomargarita sp. Thio36 draft genomes were too fragmented and thus are not included here. (**C**) Light microscopy image and model proposed for the subcellular organization in *Ca.* T. magnifica showing how the pepin organelles might develop into other cellular compartments, resulting in an increase of surface area of the bioenergetic membranes.

Dimorphic developmental cycle of Ca. T. magnifica

Laboratory observations of live *Ca.* T. magnifica revealed eventual apical bud detachment from the filament and release into the environment, likely representing a dispersive stage of the developmental cycle (Fig. 1C; fig. S1, B to F; and supplementary text). We observed dozens of cells at all intermediary stages, from the smallest attached cells resembling terminal segments recently settled to the largest filaments with apical constrictions (fig. S1 and movies S1 to S3 and S6). Such a dimorphic life cycle resembles the aquatic single-celled model system *Caulobacter crescentus*, as well as the multicellular segmented filamentous bacteria, albeit at a different scale, in which stalked "parent" cells produce free-living "daughter" cells (*35*, *36*). Because of this asymmetrical division mode, only a small fraction of the genome copies present within pepins in the most apical bud (≈1%) were transmitted to the daughter cell (fig. S9). Like the polyploid giant bacterium *Epulopiscium* spp., *Ca.* T. magnifica apparently transmits only a subset of its genomes, so-called "germline genomes," to the offspring (*14*, *24*). If terminal buds are indeed daughter cells, then such a developmental cycle may have evolved to enhance dispersion similar to the fruiting bodies of the social myxobacteria or to the aerial hyphae of *Streptomyces* spp. (*37*). This apparent life cycle is also somewhat analogous to the sulfur-oxidizing giant ciliate symbiosis, *Zoothamnium niveum* (*38*), possibly representing a case of convergent evolution of developmental cycle across domains (see the supplementary text). As with other aspects of *Ca.* T. magnifica biology, detailed investigations of cell division and its regulation will require the establishment of stable laboratory cultures, and considering the cell size, spatial omics approaches within a single cell might be tractable.

Concluding remarks

Confirmation bias related to viral size prevented the discovery of giant viruses for more than a century, and their ubiquity is only now being recognized (*39*, *40*). The discovery of *Ca.* T. magnifica suggests that large and more complex bacteria may be hiding in plain sight.

Investigating the biology, energy metabolism, and the formation, nature, and role of pepins will take us a step closer to understanding the evolution of biological complexity.

Although cells of most bacteria and archaea are ~2 μm, eukaryotic cells are usually between 10 and 20 μm, with some of the largest single-cell eukaryotes reaching 3 to 4 cm (*41*). Several theoretical frameworks explain the restriction of bacteria and archaea to microscopic sizes, including: (i) the lack of active intracellular transport and the reliance on chemical diffusion, which is efficient only along micrometer distances (*4*); (ii) a predicted maximum cell volume constraining the number of needed ribosomes should the cell grow larger (*21*); or even (iii) a decrease in energy efficiency due to mismatched surface area to volume ratio when considering placement of membrane-bound ATP synthases (*18*, *20*). These frameworks all suggest that with increasing size, the physiological or metabolic needs of a bacterial cell grow faster than the cell's capacity to sustain it and should reach a limit. The next largest prokaryote known after *Ca.* T. magnifica, *Ca.* T. nelsonii, has a metabolically active biovolume of 1.05×10^{-14} m^3 (excluding the central vacuole), close to the predicted maximum due to ribosome limitations, 1.39×10^{-15} m^3, and to the bioenergetic membrane limitation of 10^{-14} m^3 (*18*, *21*). Our precise 3D measurements on a 4.27-mm *Ca.* T. magnifica cell revealed a cytoplasm biovolume several orders of magnitude above that limit (5.91×10^{-12} m^3; table S2). It is possible that changes in spatial organization of cellular components, such as DNA and ribosome compartmentalization and rearrangement of the bioenergetic membrane system, may allow *Ca.* T. magnifica to overcome many such limitations (Fig. 3C).

Distributed in at least 23 phyla are 19 known types of bacterial organelles, of which only seven are membrane bound (*16*, *42*). Cyanobacteria can form multicellular, centimeter-long filaments and are capable of cell differentiation (*43*). Planctomycetes have special energy transduction organelles called anammoxosomes and a compartmentalized cell, and some are even capable of phagocytosis (*16*, *44*). The social Myxobacteria have large genomes and a complex developmental cycle, and are capable of moving and feeding cooperatively in predatory groups (*45*). Through its gigantic cell size, its large genome, and its dimorphic life cycle, but most importantly through its compartmentalization of genetic material in membrane-bound pepins, *Ca.* T. magnifica adds to the list of bacteria that have evolved a high level of morphological complexity. Because it segregates its genetic material in membrane-bound organelles, *Ca.* T. magnifica challenges our concept of a bacterial cell.

REFERENCES AND NOTES

1. A. D. Steen *et al.*, *ISME J.* **13**, 3126–3130 (2019).
2. D. Ionescu, M. Bizic, "Giant bacteria," in *eLS* (Wiley, 2019); https://doi.org/10.1002/9780470015902.a0020371.pub2.
3. P. A. Levin, E. R. Angert, *Cold Spring Harb. Perspect. Biol.* **7**, a019216 (2015).
4. H. N. Schulz, B. B. Jorgensen, *Annu. Rev. Microbiol.* **55**, 105–137 (2001).
5. H. N. Schulz *et al.*, *Science* **284**, 493–495 (1999).
6. E. R. Angert, K. D. Clements, N. R. Pace, *Nature* **362**, 239–241 (1993).
7. D. C. Nelson, C. O. Wirsen, H. W. Jannasch, *Appl. Environ. Microbiol.* **55**, 2909–2917 (1989).
8. M. Huettel, S. Forster, S. Kloser, H. Fossing, *Appl. Environ. Microbiol.* **62**, 1863–1872 (1996).
9. M. R. Jean *et al.*, *PLOS ONE* **10**, e0117832 (2015).
10. J. M. Larkin, M. C. Henk, *Microsc. Res. Tech.* **33**, 23–31 (1996).
11. V. Salman, J. V. Bailey, A. Teske, *Antonie van Leeuwenhoek* **104**, 169–186 (2013).
12. J. V. Bailey *et al.*, *ISME J.* **5**, 1926–1935 (2011).
13. S. Maier, H. Volker, M. Beese, V. A. Gallardo, *Can. J. Microbiol.* **36**, 438–448 (1990).
14. E. R. Angert, *Annu. Rev. Microbiol.* **66**, 197–212 (2012).
15. S. Schorn *et al.*, *FEMS Microbiol. Ecol.* **96**, fiz200 (2020).
16. C. Greening, T. Lithgow, *Nat. Rev. Microbiol.* **18**, 677–689 (2020).
17. T. Katayama *et al.*, *Nat. Commun.* **11**, 6381 (2020).
18. P. E. Schavemaker, S. A. Muñoz-Gómez, The role of mitochondrial energetics in the origin and diversification of eukaryotes. bioRxiv 465364 [Preprint] (2021); https://doi.org/10.1101/2021.10.23.465364.
19. N. Lane, *Curr. Biol.* **30**, R471–R476 (2020).
20. N. Lane, W. Martin, *Nature* **467**, 929–934 (2010).
21. C. P. Kempes, L. Wang, J. P. Amend, J. Doyle, T. Hoehler, *ISME J.* **10**, 2145–2157 (2016).
22. R. Hatzenpichler *et al.*, *Environ. Microbiol.* **16**, 2568–2590 (2014).
23. J. E. Mendell, K. D. Clements, J. H. Choat, E. R. Angert, *Proc. Natl. Acad. Sci. U.S.A.* **105**, 6730–6734 (2008).
24. E. R. Angert, *Genome Biol. Evol.* **13**, evab037 (2021).
25. D. Ionescu, M. Bizic-Ionescu, N. De Maio, H. Cypionka, H. P. Grossart, *Nat. Commun.* **8**, 455 (2017).
26. V. Salman-Carvalho, E. Fadeev, S. B. Joye, A. Teske, *Front. Microbiol.* **7**, 1173 (2016).
27. B. J. Shapiro, *Curr. Opin. Microbiol.* **31**, 116–123 (2016).
28. T. Woyke *et al.*, *PLOS ONE* **5**, e10314 (2010).
29. B. E. Flood *et al.*, *Front. Microbiol.* **7**, 603 (2016).
30. M. Winkel *et al.*, *Front. Microbiol.* **7**, 964 (2016).
31. K. Chiyomaru, K. Takemoto, *R. Soc. Open Sci.* **7**, 191859 (2020).
32. L. Katz, R. H. Baltz, *J. Ind. Microbiol. Biotechnol.* **43**, 155–176 (2016).
33. D. A. Miller, G. Suen, K. D. Clements, E. R. Angert, *BMC Genomics* **13**, 265 (2012).
34. A. J. F. Egan, J. Errington, W. Vollmer, *Nat. Rev. Microbiol.* **18**, 446–460 (2020).
35. S. A. Woldemeskel, E. D. Goley, *Trends Microbiol.* **25**, 673–687 (2017).
36. E. A. Hutchison, D. A. Miller, E. R. Angert, *Microbiol. Spectr.* **2**, 2.5.22 (2014).
37. D. Claessen, D. E. Rozen, O. P. Kuipers, L. Søgaard-Andersen, G. P. van Wezel, *Nat. Rev. Microbiol.* **12**, 115–124 (2014).
38. M. Bright, S. Espada-Hinojosa, I. Lagkouvardos, J. M. Volland, *Front. Microbiol.* **5**, 145 (2014).
39. C. Abergel, M. Legendre, J. M. Claverie, *FEMS Microbiol. Rev.* **39**, 779–796 (2015).
40. F. Schulz *et al.*, *Nature* **578**, 432–436 (2020).
41. J. Dumais, K. Serikawa, D. F. Mandoli, *J. Plant Growth Regul.* **19**, 253–264 (2000).
42. C. A. Kerfeld, C. Aussignargues, J. Zarzycki, F. Cai, M. Sutter, *Nat. Rev. Microbiol.* **16**, 277–290 (2018).
43. E. Flores, A. Herrero, *Nat. Rev. Microbiol.* **8**, 39–50 (2010).
44. T. Shiratori, S. Suzuki, Y. Kakizawa, K. I. Ishida, *Nat. Commun.* **10**, 5529 (2019).
45. J. Muñoz-Dorado, F. J. Marcos-Torres, E. García-Bravo, A. Moraleda-Muñoz, J. Pérez, *Front. Microbiol.* **7**, 781 (2016).
46. R. M. Bowers *et al.*, *Nat. Biotechnol.* **35**, 725–731 (2017).

ACKNOWLEDGMENTS

We are thankful to the following centers where the electron microscopy analyses were performed: the Centre Commun de Caractérisation des Matériaux des Antilles et de la Guyane in Guadeloupe, F.W.I., which is supported by The European Regional Development Fund, the Regional Council of Guadeloupe, and the French Research Department; the Electron Microscope Lab (EML) of the University of California Berkeley; the Electron Microscopy Resource in Donner at LBNL, Berkeley; and the FEI Eindhoven Center. We are particularly grateful to D. Jorgens at EML for advice and assistance in electron microscopy sample preparation and data collection. The x-ray tomography data were acquired at the Stanford Nano Shared Facilities at Stanford University (Palo Alto, CA), and we are particularly grateful to A. Vailionis for his technical support during hard x-ray tomography scan acquisitions. The confocal microscopy observations were performed at the Advanced Microscopy Facility at LBNL (Berkeley, CA). Preliminary confocal microscopy observations were acquired at the IBPS Imaging Facility, which is supported by "Conseil Regional d'Ile-de-France." We thank S. Volland for his help with 3D rendering animations and H. Maughan for copyediting this manuscript. The work (proposal: 10.46936/10.25585/60001074) conducted by the US Department of Energy Joint Genome Institute (https://ror.org/04xm1d337), a Department of Energy (DOE) Office of Science User Facility, is supported by the Office of Science of the DOE operated under contract no. DE-AC02-05CH11231. The Nagoya permit TREL1820249A/50 (unique identifier ABSCH-IRCC-FR-246822-1) can be consulted publicly online at: https://absch.cbd.int/en/search. **Funding:** This work was supported by the John Templeton Foundation (grant 60973 to J.-M.V., S.V.D., and T.T.), the Gordon and Betty Moore Foundation (grant GBMF7617 to J.-M.V., S.V.D., and T.T.), DARPA (award no. HR001120036 to J.-M.V., S.V.D., and T.T.); the DOE Office of Science (contract no. DE-AC02-05CH11231 to T.W., F.S., T.T., J.-M.V., K.M.D., and N.H.E.), and Region Guadeloupe (F.W.I. grant to M.R.J.). **Author contributions:** Conceptualization: O.G., S.G.R., J.-M.V., T.W., S.V.D., F.S., R.R.M., N.I., T.T., N.H.E.; Data curation: N.I., F.S., J.-M.V., D.U., S.G.R.; Formal analysis: J.-M.V., S.G.R., F.S., N.I., D.U., O.G.; Funding acquisition: T.W., S.V.D., O.G., J.L.M.; Investigation: J.-M.V., S.G.R., O.G., T.T., F.S., D.U., D.G., N.N., N.I., C.G.R., S.B.K., N.H.E., M.R.J., J.L.M.; Methodology: O.G., T.T., J.-M.V., S.V.D., S.G.R., D.G., N.N., R.R.M., T.W., C.G.R., S.B.K.; Resources: K.M.D., T.W., R.R.M., O.G., J.L.M., N.H.E., N.J.M.; Supervision: O.G., T.W., S.V.D.; Visualization: O.G., S.G.R., J.-M.V., F.S., N.I., D.U.; Writing – original draft: J.-M.V.; Writing – review and editing: J.-M.V., S.G.R., O.G., T.W., S.V.D., E.A., N.I., R.R.M. **Competing interests:** S.V.D. serves as the CEO of Sample Exchange. The remaining authors declare no competing interests. **Materials and data availability:** All data needed to evaluate the conclusions in this study are present in the main manuscript or the supplementary materials. The complete assemblies as well as the extracted *Ca.* T. magnifica draft genomes have been deposited in IMG (https://img.jgi.doe.gov/). The raw reads have been deposited in SRA (https://www.ncbi.nlm.nih.gov/sra). Accession numbers are provided in tables S3 and S4.

SUPPLEMENTARY MATERIALS

science.org/doi/10.1126/science.abb3634
Materials and Methods
Supplementary Text
Figs. S1 to S20
Tables S1 to S11
References (*47*–*83*)
Movies S1 to S6
MDAR Reproducibility Checklist

View/request a protocol for this paper from *Bio-protocol*.

Submitted 16 October 2021; resubmitted 26 March 2022
Accepted 9 May 2022
10.1126/science.abb3634